Available online at www.sciencedirect.com
SCIENCE DIRECT®
Life Sciences 78 (2006) 2734 – 2741
Life Sciences
www.elsevier.com/locate/lifescie

Changes of cerebral blood oxygenation and optical pathlength during activation and deactivation in the prefrontal cortex measured by time-resolved near infrared spectroscopy

Kaoru Sakatani [a,b,c,*], Daisuke Yamashita [d], Takeshi Yamanaka [d], Motoki Oda [d], Yutaka Yamashita [d], Tetsuya Hoshino [a], Norio Fujiwara [a], Yoshihiro Murata [a,b], Yoichi Katayama [a,c]

[a] *Department of Neurological Surgery, Nihon University School of Medicine, Japan*
[b] *Division of Optical Brain Engineering, Nihon University School of Medicine, Japan*
[c] *Division of Applied System Neuroscience, Nihon University School of Medicine, Japan*
[d] *Central Laboratory, Hamamatsu Photonics K.K., Japan*

Received 1 June 2005; accepted 26 October 2005

Abstract

To determine the alterations in optical characteristics and cerebral blood oxygenation (CBO) during activation and deactivation, we evaluated the changes in mean optical pathlength (MOP) and CBO induced by a verbal fluency task (VFT) and driving simulation in the right and left prefrontal cortex (PFC), employing a newly developed time-resolved near infrared spectroscopy, which allows quantitative measurements of the evoked-CBO changes by determining the MOP with a sampling time of 1 s. The results demonstrated differences in MOP in the foreheads with the subjects and wavelength; however, there was no significant difference between the right and left foreheads ($p > 0.05$). Also, both the VFT and driving simulation task did not affect the MOP significantly as compared to that before the tasks ($p > 0.05$). In the bilateral PFCs, the VFT caused increases of oxyhemoglobin and total hemoglobin associated with a decrease of deoxyhemoglobin, while the driving simulation task caused decreases of oxyhemoglobin and total hemoglobin associated with an increase of deoxyhemoglobin; there were no significant differences in evoked-CBO changes between the right and left PFC. The present results will be useful for quantitative measurement of hemodynamic changes during activation and deactivation in the adults by near infrared spectroscopy.

Keywords: BOLD; Deactivation; NIRS; Prefrontal cortex; Driving; Frontal lobe

Introduction

Blood oxygenation level dependent (BOLD) contrast functional MRI (fMRI) detects neuronal activity by measuring changes in BOLD signal (i.e. T_2* signal), which is caused by concentration changes of deoxyhemoglobin (HHb) in the cerebral vessels (Ogawa et al., 1990, 1992). It is believed that an increase in BOLD signal reflects a focal increase of neuronal activity, while a decrease in BOLD signal, so-called "deactivation", reflects a focal suppression of neuronal activity (Fransson et al., 1999; Reynolds et al., 1988). However, near infrared spectroscopy (NIRS) studies on newborn infants have demonstrated that neuronal activation causes an increase of HHb concentration associated with increases of oxyhemoglobin (O_2Hb) and total hemoglobin (tHb) (Meek et al., 1998; Sakatani et al., 1999a,b,c,d). Such atypical evoked cerebral blood oxygenation (CBO) changes were observed in the activated motor cortex of patients with brain disorders (Fujiwara et al., 2004; Murata et al., 2002, 2004; Sakatani et al., 1988). In addition, the BOLD signal decreases in these areas (Born et al., 1996; Murata et al., 2004). These findings suggest that the BOLD signal could decrease not only in deactivated areas but also in activated areas, which BOLD–fMRI alone cannot distinguish from one another.

NIRS is an optical method for measuring concentration changes of oxyhemoglobin (O_2Hb) and HHb in the cerebral

* Corresponding author. Department of Neurological Surgery, Division of Optical Brain Engineering, Nihon University School of Medicine, 30-1, Oyaguchi-Kamimachi, Itabashi-ku, Tokyo 173-8610, Japan. Tel.: +81 3 3972 8111x2481; fax: +81 3 3554 0425.
E-mail address: sakatani@med.nihon-u.ac.jp (K. Sakatani).

0024-3205/$ - see front matter © 2005 Elsevier Inc. All rights reserved.
doi:10.1016/j.lfs.2005.10.045

vessels by means of the characteristic absorption spectra of hemoglobin in the near infrared range (Jöbsis, 1977; Reynolds et al., 1988). Changes in total hemoglobin (sum of O_2Hb and HHb; tHb) indicate cerebral blood volume changes and correlate with regional cerebral blood flow (rCBF) changes under conditions of constant hematocrit and perfusion pressure (Ferrari et al., 1992; Pryds et al., 1990). In addition, it was demonstrated that changes in O_2Hb correlated with changes in rCBF in the perfused rat brain model (Hoshi et al., 2001). NIRS thus provides more information about the evoked-CBO changes than does BOLD-fMRI, although the spatial resolution of NIRS is poor due to light scattering within the tissues. NIRS has been applied for the evaluation of evoked-CBO changes in normal adults (Hock et al., 1995; Hoshi and Tamura, 1993; Hoshi, 2003; Kato et al., 1993; Kleinschmidt et al., 1996; Sakatani et al., 1988; Tanida et al., 2004), newborn infants (Meek et al., 1998; Sakatani et al., 1999a,b,c,d) and patients with brain disorders (Fujiwara et al., 2004; Murata et al., 2002, 2004; Sakatani et al., 1988, 1999a,b,c,d).

NIRS is based on the modified Beer-Lambert law, in which changes in hemoglobin chromophore concentrations are assumed to be proportional to changes in light absorbance divided by the extinction coefficients of the chromophores and the mean optical pathlength (MOP) in the tissue, which is the average distance that light travels between the source and detector through the tissue (Delpy et al., 1988). For the measurement of absolute values of the hemoglobin chromophore concentration changes, it is necessary therefore to determine the MOP, which can be estimated by a time-resolved or frequency domain NIRS. In many activation studies employing continuous wave NIRS, the MOP has been assumed to be constant among the subjects (Fujiwara et al., 2004; Hock et al., 1995; Kato et al., 1993; Kleinschmidt et al., 1996; Meek et al., 1998; Murata et al., 2002, 2004; Sakatani et al., 1988, 1999a,b,c,d; Tanida et al., 2004); however, the MOP may vary among the subjects because of individual differences in thickness of the extracranial and intracranial tissues. Indeed, a time-resolved NIRS has demonstrated differences in MOP with the subjects, regions of the head, and wavelength (Zhao et al., 2002). In addition, hemodynamic changes in the cerebral tissue during activation and deactivation could alter the MOP. It is not yet clear, however, whether the MOP does change or not during activation and deactivation because the time-resolved NIRS does not permit real time measurements of the MOP due to their slow data collection rate and long computation time (Hoshi, 2003; Zhao et al., 2002).

In the present study, we evaluated the changes in CBO and optical pathlength during activation and deactivation in the prefrontal cortex (PFC), using a newly developed time-resolved NIRS, which allows measurements of O_2Hb and HHb changes by determining the MOP with a high time resolution (i.e. 1 s). We employed a verbal fluency task (VFT) for activation of the PFC. BOLD-fMRI demonstrated increases of the BOLD signal in the PFC during the VFT (Binder et al., 1997), while NIRS has demonstrated an increase of O_2Hb and tHb associated with a decrease of HHb in the PFC during the VFT (Fallgatter et al., 1997; Herrmann et al., 2003; Sakatani et al., 1988, 1999b). Recently, time-resolved NIRS demonstrated similar evoked-CBO changes in the PFC (Quaresima et al., 2005). In addition, we employed the driving simulation task for deactivation of the PFC. Although NIRS has not been employed to evaluated the evoked-CBO changes during driving simulation, BOLD-fMRI demonstrated negative BOLD signal changes in several brain regions including the PFC (Calhoun et al., 2002).

Subjects and methods

Subjects

We investigated seven normal adult subjects (six men and one woman; mean age, 33.1±8.6 years (mean±SD); range, 22–47 years) in the present study. The subjects were highly educated in Japanese with an average of 16.8±1.0 years of schooling (range, 16–18 years). All of the subjects were accustomed to driving a car, with an average of 12.8±8.5 years of driving experience (range, 3–28 years); however, they had only limited experience of playing computer games. The study was approved by the Committee for Clinical Trials and Research on Humans of Nihon University School of Medicine, and informed consent to participate in the study was obtained from each subject.

Tasks

We used a commercially available PC game (SIDE-by-SIDE Special, TAITO Co., Tokyo) for the driving simulation. The course consisted of circling through a virtual island in the absence of any traffic, with the road and scenery along the roadside changing continuously. A joystick was employed to control the car movements; the subjects could adapt to the use of the joystick after a brief training period. During the driving simulation, subjects were instructed to drive safely but as fast as possible.

We chose the VFT, which entails naming as many animals or fruits as possible, as the language task; the VFT is a well-established neuropsychological test of frontal lobe function (Lezak, 1995) that has been shown to activate the PFC in several activation studies using fMRI (Binder et al., 1997), PET (Parks et al., 1988) and NIRS (Fallgatter et al., 1997; Herrmann et al., 2003; Sakatani et al., 1988, 1999b).

After a baseline measurement lasting 120 s, the subjects performed the VFT for 60 s followed by 120 s recovery. They then performed driving simulation for 60 s followed by 120 s recovery.

NIRS

Our new system was essentially a multi-channel time-resolved spectroscopic system employing pulsed-laser diodes and time-correlated single photon counters as shown in Fig. 1. Three semiconductor laser diodes (NLP, nanosecond light pulsers) were used as the light source. They emit near-infrared

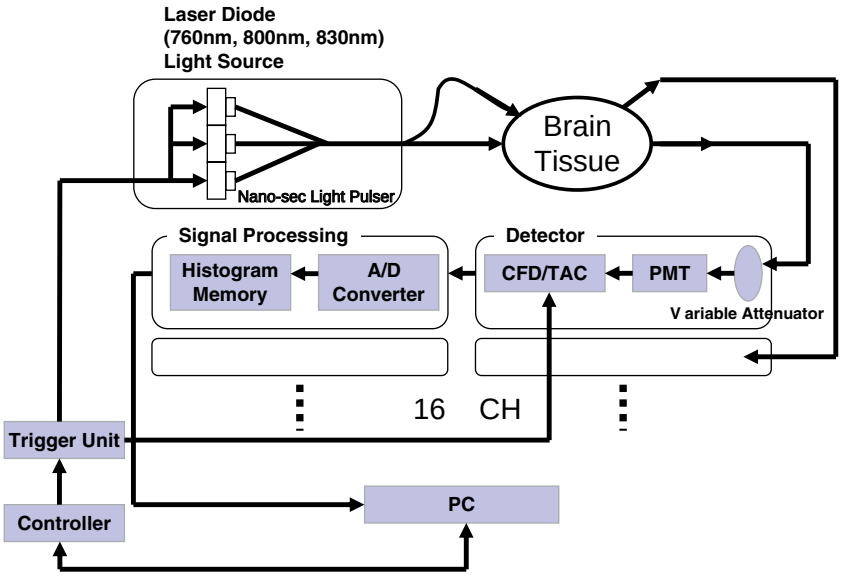

Fig. 1. Block diagram of the time-resolved NIRS. PMT = photomultiplier tube, AMP = amplifier, CFD = constant fraction discriminator, TAC = time-to-amplitude converter.

pulsed light with a pulse duration at each wavelength of about 1 ns, and driven at a frequency of 5 MHz. Their wavelengths were 760, 800, and 830 nm, respectively. The outputs of these three pulse lasers were first integrated by an optical fiber coupler, and then split by the optical fiber coupler according to the number of sites that must be irradiated. The average power of the irradiation light for all of the light wavelengths at the irradiation sites was about 140 μW.

The diffuse reflected light from the target was picked up by a coaxial bundle fiber and photo-detector unit. The structure of the coaxial fiber was such that the irradiation light passed through the inner fiber and the detected light returned via the fiber in the annulus. The diameter of the bundle fiber was 3 mm. Employment of a fiber optic switch which could select the light source position on the object, enabled multi-point measurement for the reconstruction image. The detector system had 16 completely independent channels of time-correlated single photon counting for time-resolved measurements. These channels were synchronized. One channel consisted of an optical attenuator, a highly sensitive and fast PMT (photomultiplier tube), a fast AMP (amplifier), a CFD (constant fraction discriminator), a TAC (time-to-amplitude converter), an A/D converter, and a signal acquisition unit. The CFD picked up the photon pulses from the PMT, and the TAC generated a voltage proportional to the time of flight of the photons. The signal acquisition unit produced a histogram showing the rate of occurrence of photon pulses falling within a specified time range. The time resolution of the system was about 25 ps.

Employing the two channels of the system, we measured changes in the evoked CBO and MOP in the bilateral PFC simultaneously. The optodes were placed at a distance of 3 cm on the bilateral forehead; the center of the 2 optodes was identical to the Fp2 position of the internal EEG 10–20 system. MRI with the use of vitamin E capsules confirmed that the optodes were placed over the PFC.

Data analysis

The mean time of flight $\langle t\rangle$ was obtained by subtracting the gravity of the instrumental function $\langle t\rangle_{\mathrm{i}}$ from those of the observed temporal profiles $\langle t\rangle_{\mathrm{o}}$ (Zhang et al., 1998). If we assume the speed of photons c is constant in the tissue (refractive index of the tissue was assumed to be 1.3.), the mean optical pathlength MOP can be calculated as follows:

$$\mathrm{MOP} = c\cdot\langle t\rangle = c\cdot\left(\langle t\rangle_{\mathrm{o}} - \langle t\rangle_{\mathrm{i}}\right) = c\cdot\left\{\frac{\sum_{k=0}^{N} k\ O(k)\ T}{\sum_{k=0}^{N} k\ O(k)} - \frac{\sum_{k=0}^{N} k\ I(k)\ T}{\sum_{k=0}^{N} I(k)}\right\} \quad (1)$$

where N is the total number of time steps in the time axis of the temporal profile, $O(k)$ is the photon count of the observed temporal profile at the kth time interval, and T is the time interval, which was about 25 ps for the present system. $I(k)$ is the photon count of the instrumental function at the kth time interval.

The calculation of the hemoglobin concentrations was based on the modified Beer-Lambert law and can be written as

$$\Delta\mathrm{OD}^{\lambda} = -\log\frac{I_2^{\lambda}}{I_1^{\lambda}} = \left(\varepsilon^{\lambda}_{\mathrm{O_2Hb}}\Delta[\mathrm{O_2Hb}] + \varepsilon^{\lambda}_{\mathrm{HHb}}\Delta[\mathrm{HHb}]\right)\mathrm{MOP}^{\lambda} \quad (2)$$

where λ is the NIR light wavelength used in the measurement, ΔOD is the change of optical density, which is the logarithm of the ratio between the two intensities before (I_1) and after (I_2) the change, and $\varepsilon_{\mathrm{O_2}}\mathrm{Hb}$ and $\mathring{a}_{\mathrm{HHb}}$ are the extinction coefficients of O_2Hb and HHb, respectively (Cope, 1991).

Table 1
Mean optical pathlength at 760, 800, and 830 nm before and during the verbal fluency task (VFT) and driving simulation task in the right and left PFC

	Left			Right		
	760 nm	800 nm	830 nm	760 nm	800 nm	830 nm
Control	17.3±0.1	17.3±0.1	15.2±0.2[a]	17.0±0.1	17.1±0.1	14.9±0.2[b]
VFT	17.3±0.1	17.2±0.1	15.4±0.2[a]	17.0±0.1	16.9±0.1	14.7±0.2[b]
Driving simulation	17.3±0.1	17.3±0.1	15.3±0.2[a]	17.1±0.1	17.1±0.1	14.9±0.2[b]

Data are expressed as the means±SD (cm).
[a] $p<0.01$ vs. 760, 800 nm ($F=7$).
[b] $p<0.02$ vs. 760, 800 nm ($F=7$).

We analyzed the concentration changes in O_2Hb, HHb, and tHb by subtracting the mean control values (averaged value during 60 s) from the mean activation values (averaged value during 60 s). We employed a paired *t*-test for comparison of the control values and activation values during the VFT and driving simulation. In addition, we employed a Wilcoxon signed-rank test for comparison of the activation values during the VFT and driving simulation.

Results

Optical pathlength

The time-resolved NIRS could measure the MOP continuously before and during the tasks. Table 1 summarizes the average values of the measured MOP in the bilateral foreheads before and during the tasks at 760, 800 and 830 nm. In the control condition, the MOP of the left forehead varied from 15.0 to 19.2 cm at 760 nm, from 14.9 to 19.3 cm at 800 nm, and from 12.9 to 17.2 cm at 830 nm, while the MOP of the right forehead varied from 15.0 to 18.5 cm at 760 nm, from 14.7 to 18.3 cm at 800 nm, and from 12.4 to 16.2 cm at 830 nm. There was no significant difference in MOP between the right and left foreheads ($p>0.05$). A wavelength dependence of the MOP, involving a decrease by about 13% with an increase in wavelength from 760 nm to 830 nm, was noted in the bilateral foreheads.

Fig. 2 shows a typical example of the changes in MOP at each wavelength during the course of the experiments. Although fluctuations of the MOP were observed before and during the tasks, the standard deviations of the MOP changes were only less than 0.2 cm. Overall, both the VFT and driving simulation task did not affect the MOP significantly as compared to that before the tasks (Table 1).

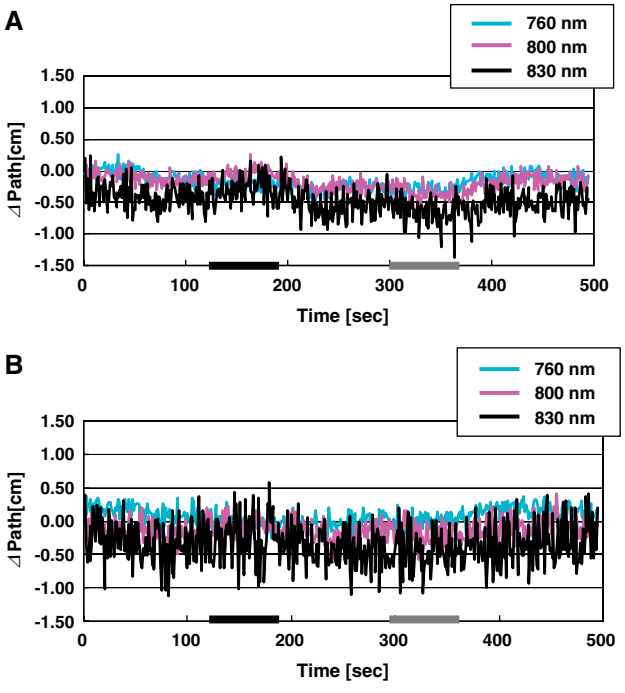

Fig. 2. Typical example of the changes in mean optical pathlength (MOP) at 760, 800, and 830 nm in the right (A) and left (B) foreheads during the course of the experiments. The MOP at 760, 800, and 830 nm before the tasks was 16.3, 16.8, and 15.3 cm, respectively. Small fluctuations of the MOP (SD<0.2 cm) were observed before and during the tasks; however, both the VFT and driving simulation task failed to affect the MOP significantly as compared to that before the tasks.

CBO changes during the VFT and driving simulation

In all subjects, the VFT and driving simulation task significantly altered the CBO in the bilateral PFC; however, the pattern of NIRS parameter changes induced by the VFT differed from that induced by the driving simulation task. The

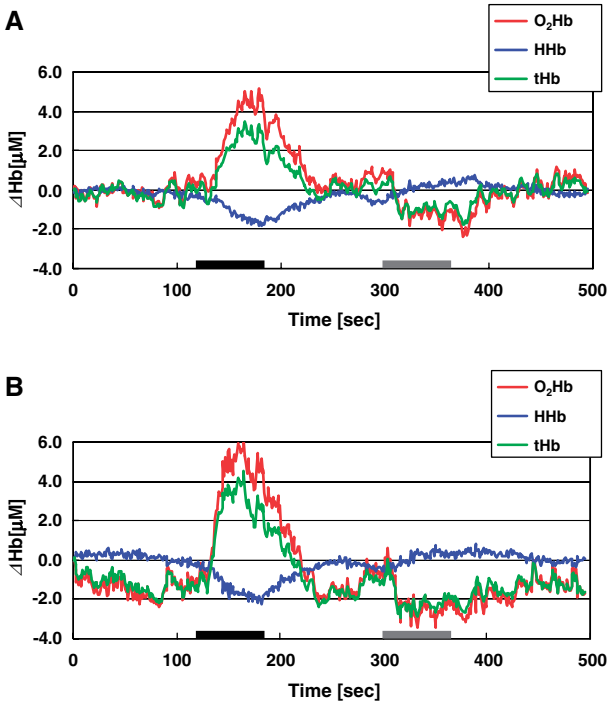

Fig. 3. Typical example of the CBO changes the right (A) and left (B) PFC during the course of the experiments (same subject as in Fig. 2). The ordinates indicate the concentration changes of O_2Hb (pink lines), HHb (blue lines), and tHb (black lines) in ìM. The thick bars below the NIRS parameter changes indicate the periods of the tasks. The VFT (black bar) caused increases of O_2Hb and tHb associated with a decrease of HHb, while driving simulation task (gray bar) caused decreases of O_2Hb and tHb associated with an increase of HHb. (For interpretation of the references to colour in this figure legend, the reader is referred to the web version of this article.)

Table 2
CBO changes during the verbal fluency task (VFT) and driving simulation task in the right and left PFC

	Left			Right		
	O_2Hb	HHb	tHb	O_2Hb	HHb	tHb
VFT	4.1±5.7	−1.0±0.6	3.1±5.1	4.3±5.7	−1.0±0.6	3.4±5.1
Driving simulation	−1.4±2.3[a]	0.2±0.8[b]	−1.2±1.6[c]	−1.2±2.7[d]	0.3±0.7[e]	−0.7±2.2[f]

Data are expressed as the means±SD(μM).
[a] $p<0.05$ vs. VFT.
[b] $p<0.01$ vs. VFT.
[c] $p<0.05$ vs. VFT.
[d] $p<0.05$ vs. VFT.
[e] $p<0.01$ vs. VFT.
[f] $p<0.05$ vs. VFT.

VFT caused increases of O_2Hb and tHb associated with a decrease of HHb. In contrast, the driving simulation task caused decreases of O_2Hb and tHb associated with an increase of HHb. These CBO changes induced by the tasks returned to the control level during the recovery phase. Fig. 3 shows a typical example of the CBO changes during the course of the experiments. There were significant differences in O_2Hb ($p<0.05$, $T=1$ in the right and left PFC), HHb ($p<0.01$, $T=0$ in the right and left PFC), and tHb ($p<0.05$, $T=2$ in the left PFC; $p<0.05$, $T=4$ in the right PFC) between the VFT and driving simulation (Table 2). In contrast, there were no significant differences in the CBO changes during the VFT and driving simulation between the right and left PFC.

Discussion

Optical pathlength before and during the tasks

The present results demonstrated differences in MOP in the foreheads with the subjects and wavelength. The optical differential pathlength factors (DPF) at 760, 800, and 830 nm, which were calculated from the measured MOP (i.e. DPF = MOP/3 cm optode separation), were 5.8, 5.8 and 5.1, respectively. These values and the wavelength dependence of the DPF are consistent with results obtained previously by time-resolved NIRS (Zhao et al., 2002) and frequency-modulated NIRS (Duncan et al., 1995). The individual differences in the MOP indicate that continuous wave NIRS which employs a uniform MOP may not allow accurate quantitative measurements of CBO changes because the MOP variation directly affects the calculation of the hemoglobin concentration changes (Eq. (2)).

The present time-resolved NIRS allowed measurements of the MOP changes during tasks with a sampling time of 1 s. We observed no significant changes in MOP at each wavelength during the tasks, although there were small fluctuations of the MOP (SD < 0.2 cm). The MOP is determined by scattering and absorption in the tissue; an increase in scattering increases MOP while an increase in absorption decreases MOP (Patterson et al., 1986). Therefore, if both scattering and absorption in the brain tissue increase simultaneously, or if they decrease simultaneously, there is a possibility that MOP may not change. To clarify the activity-dependent changes in scattering and absorption, it is necessary to evaluate the reduced scattering and absorption coefficients by fitting the analytical solution of the photon diffusion equation to the measured time-resolved reflectance curve (Gratton and Fabiani, 2003; Wolf et al., 2003). In the present study, however, we did not employ this approach, because it reduces the sampling time. Further studies are necessary to clarify the activity-dependent changes in scattering and absorption in the human brain.

CBO changes during activation in the PFC

Employing the time-resolved NIRS, we were able to measure changes of O_2Hb and HHb in the PFC quantitatively by determining the MOP during the VFT. The time-resolved NIRS revealed that the VFT caused increases of O_2Hb and tHb associated with a decrease of HHb, findings which are consistent with those obtained by continuous wave NIRS (Fallgatter et al., 1997; Herrmann et al., 2003; Sakatani et al., 1988, 1999b) and time resolved NIRS (Quaresima et al., 2005); the increase in O_2Hb indicates rCBF rises in the activated area, while the decrease in HHb is caused by a large increase of rCBF which exceeds the increase in oxygen consumption during activation (Fox and Raichle, 1986). The changes in O_2Hb, HHb and tHb were expressed as absolute values; however, these NIRS parameter changes reflect the average changes of the CBO within the illuminated area, which is much larger than the voxel size of PET or fMRI. Thus, the NIRS parameter changes indicated the average CBO changes in that part of the PFC through which the NIR light passed.

The VFT caused evoked-CBO changes in the bilateral PFC, which is located outside the classical “Broca’s area”. fMRI studies have demonstrated similar activated areas outside Broca’s area during language tasks, suggesting that the activation induced by the VFT may reflect the executive component of the VFT more than language specific activation (Binder et al., 1997). Employing continuous wave NIRS, VFT-induced CBO changes have been compared between the right and the left PFC; the results obtained by continuous wave NIRS were, however, controversial (Fallgatter et al., 1997; Herrmann et al., 2003). It remains

unknown whether there were no significant differences in MOP of the subjects examined in these studies. In the present study, employing time-resolved NIRS, we measured quantitative changes in the CBO during the VFT by determining the MOP of the bilateral foreheads. On this basis, we were able to conclude that there was no significant difference in the VFT-induced CBO changes in the right and left PFC.

CBO changes during deactivation in the PFC

In contrast to the VFT, the driving simulation task caused an increase of HHb associated with decreases of O_2Hb and tHb; these changes were thus opposite in direction to those induced by the VFT. As increase of HHb was evident during the entire course of the task, so that it differed from the HHb rise occurring within a few seconds after the start of neuronal activation (Malonek and Grinvald, 1996), or the "post-stimulus overshoot" of HHb occurring in the visual cortex (Heekeren et al., 1997). The decreases of O_2Hb and tHb implied a decrease of rCBF in response to the task. These findings strongly suggest that driving simulation caused deactivation in the PFC, since an increase of HHb (which is paramagnetic) give rise to a decrease of BOLD signal (Ogawa et al., 1990, 1992). Indeed, Calhoun et al. have demonstrated decreases of BOLD signals in the PFC during driving simulation; the decrease in BOLD signal was correlated with the driving speed and implicated with vigilance (Calhoun et al., 2002). In contrast, Walter et al., employing BOLD fMRI, detected activated areas in multiple brain regions such as the sensorimotor cortex, visual cortex and cerebellum during driving simulation, but failed to observe both activation and deactivation in the PFC (Walter et al., 2001); however, deactivation can be overlooked when activation maps are calculated using software which images the activation areas by detecting only increases of the BOLD signal (Fujiwara et al., 2004; Murata et al., 2002, 2004).

It should be emphasized that a decrease of BOLD signal does not necessarily mean a decrease of the rCBF that is caused by decrements in the focal neuronal activities. For example, in the visual cortex of newborn infants, photic stimulation induced sustained decreases of BOLD signal in the visual cortex (Born et al., 1996), while NIRS revealed increases of O_2Hb and tHb during activation (Meek et al., 1998). Recently, we have demonstrated similar CBO changes associated with a decrease of BOLD signal in the activated motor cortex of a patient with a brain tumor (Murata et al., 2004). Such pseudo-deactivation cannot be distinguished from true deactivation by BOLD-fMRI alone, since the BOLD signal reflects mainly the concentration changes in HHb (Ogawa et al., 1990, 1992).

The physiological mechanism of deactivation in the PFC during driving simulation remains unclear. However, the following mechanisms warrant consideration. First, a stealing of blood from less active regions into the most CBF-demanding area could induce deactivation (Harel et al., 2002). However, this seems unlikely because BOLD-fMRI demonstrated no activated area in the PFC during driving simulation (Calhoun et al., 2002; Walter et al., 2001). Second, a suppression of neuronal activities could reduce the rCBF, resulting in an increase of HHb. Raichle et al. proposed that such a reduction of neuronal activities might be mediated through the action of diffuse projecting systems like dopamine or a reduction in thalamic inputs to the cortex during attention-demanding cognitive tasks (Raichle et al., 2001). In addition, Hinterberger et al. reported that self generation of positive slow cortical potentials caused a decrease of BOLD signal in the PFC (Hinterberger et al., 2003). These findings suggest that a depression of neuronal activity in the PFC causes a decrease of BOLD signal. Simultaneous measurements by NIRS, fMRI and electrophysiological monitoring may help to clarify the exact physiological mechanism of deactivation in the PFC.

In summary, the present study demonstrated that the newly developed time-resolved NIRS allowed measurements of evoked-CBO changes and MOP changes in the bilateral PFC with a sampling time of 1 s. The VFT caused an activation pattern (i.e. increases of O_2Hb and tHb with a decrease of HHb), while driving simulation caused a deactivation pattern (i.e. decreases of O_2Hb and tHb with an increase of HHb). There were no significant differences in evoked-CBO changes between the right and left PFC. In addition, the VFT and driving simulation caused no significant changes in the MOP in the bilateral foreheads.

Acknowledgments

This work was supported by Grants-in-Aid from the Ministry of Education, Culture, Sports, Sciences and Technology of Japan (A12307029, A15209047, C15591553, and a grant for the promotion of industry–university collaboration at Nihon University) and by Hamamatsu Photonics K.K. (Hamamatsu, Japan).

References

Binder, J.R., Frost, J.A., Hammeke, T.A., Cox, R.W., Rao, S.M., Prieto, T., 1997. Human brain language areas identified by functional magnetic resonance imaging. Journal of Neuroscience 17, 353–362.

Born, P., Rostrup, E., Leth, H., Leth, H., Peitersen, B., Lou, H.C., 1996. Changes of visually induced cortical activation patterns during development. Lancet 347, 543.

Calhoun, V.D., Pekar, J.J., McGinty, V.B., Adali, T., Watson, T.D., Pearlson, G.D., 2002. Different activation dynamics in multiple neural systems during simulated driving. Human Brain Mapping 17, 141–142.

Cope, M., 1991. The application of near infrared spectroscopy to noninvasive monitoring of cerebral oxygenation in the newborn infant, PhD Thesis, University of London.

Delpy, D.T., Cope, M., van der Zee, P., Arridge, S., Wray, S., Wyatt, J., 1988. Estimation of optical pathlength through tissue from direct time of flight measurement. Physics in Medicine and Biology 33, 1433–1442.

Duncan, A., Meek, J.H., Clemence, M., Elwell, C.E., Tyszcauk, L., Cope, M., Delpy, D.T., 1995. Optical pathlength measurements on adult head, calf and forearm and the head of the newborn infant using phase resolved optical spectroscopy. Physics in Medicine and Biology 40, 295–304.

Fallgatter, A.J., Roesler, M., Sitzmann, L., Heidrich, A., Mueller, T.J., Strik, W.K., 1997. Loss of functional hemispheric asymmetry in Alzheimerfs dementia assessed with near-infrared spectroscopy. Cognitive Brain Research 6, 67–72.

Ferrari, M., Wilson, D.A., Hanley, D.F., Traystman, R.J., 1992. Effects of graded hypotension on cerebral blood flow, blood volume, and mean transit time in dogs. American Journal of Physiology 262, 1908–1914.

Fox, P.T., Raichle, M.E., 1986. Focal physiological uncoupling of cerebral blood flow and oxidative metabolism during somatosensory stimulation in human subjects. Proceedings of the National Academy of Sciences of the United States of America 83, 1140–1144.

Fransson, P., Kruger, G., Merboldt, K.D., Frahm, J., 1999. MRI of functional deactivation: temporal and spatial characteristics of oxygenation-sensitive responses in human visual cortex. NeuroImage 9, 611–618.

Fujiwara, N., Sakatani, K., Katayama, Y., Murata, Y., Hoshino, T., Fukaya, C., Yamamoto, T., 2004. Evoked-cerebral blood oxygenation changes in false-negative activations in BOLD contrast functional MRI of patients with brain tumors. NeuroImage 21, 1464–1471.

Gratton, G.., Fabiani, M., 2003. The event-related optical signal (EROS) in visual cortex: replicability, consistency, localisation, and resolution. Psychophysiology 40, 567–571.

Harel, N., Lee, S.P., Nagaoka, T., Kim, D.S., Kim, S.G., 2002. Origin of negative blood oxygenation level-dependent fMRI signals. Journal of Cerebral Blood Flow and Metabolism 22, 908–917.

Heekeren, H.R., Obrig, H., Wenzel, R., Eberle, K., Ruben, J., Villringer, K., Kurth, R., Villringer, A., 1997. Cerebral haemoglobin oxygenation during sustained visual stimulation: a near-infrared spectroscopy study. Philosophical Transactions of the Royal Society of London. Series B, Biological Sciences 352, 743–750.

Herrmann, M.J., Ehlis, A.C., Fallgatter, A.J., 2003. Frontal activation during a verbal-fluency task as measured by near-infrared spectroscopy. Brain Research Bulletin 61, 51–56.

Hinterberger, T., Veit, R., Strehl, U., Trevorrow, T., Erb, M., Kotchoubey, B., Flor, H., Birbaumer, N., 2003. Brain areas activated in fMRI during self-regulation of slow cortical potentials (SCPs). Experimental Brain Research 152, 113–122.

Hock, C., Müller-Spahn, F., Schuh-Hofer, S., Hofmann, M., Dirnagl, U., Villringer, A., 1995. Age dependency of changes in cerebral hemoglobin oxygenation during brain activation: a near-infrared spectroscopy study. Journal of Cerebral Blood Flow and Metabolism 15, 1103–1108.

Hoshi, Y., 2003. Functional near-infrared optical imaging: utility and limitations in human brain mapping. Psychophysiology 40, 511–520.

Hoshi, Y., Tamura, M., 1993. Detection of dynamic changes in cerebral oxygenation coupled to neuronal function during mental work in man. Neuroscience Letters 150, 5–8.

Hoshi, Y., Kobayashi, N., Tamura, M., 2001. Interpretation of near-infrared spectroscopy signals: a study with a newly developed perfused rat brain model. Journal of Applied Physiology 90, 1657–1662.

Jöbsis, F.F., 1977. Noninvasive, infrared monitoring of cerebral and myocardial oxygen sufficiency and circulatory parameters. Science 198, 1264–1267.

Kato, T., Kamei, A., Takashima, S., Ozaki, T., 1993. Human visual cortical function during photic stimulation monitoring by means of near-infrared spectroscopy. Journal of Cerebral Blood Flow and Metabolism 13, 516–520.

Kleinschmidt, A., Obrig, H., Requardt, M., Merboldt, K.D., Dirnagl, U., Villringer, A., Frahm, J., 1996. Simultaneous recording of cerebral blood oxygenation changes during human brain activation by magnetic resonance imaging and near-infrared spectroscopy. Journal of Cerebral Blood Flow and Metabolism 16, 817–826.

Lezak, M.D., 1995. Neuropsychological Assessment, Third edition. Oxford University Press, New York.

Malonek, D., Grinvald, A., 1996. Interactions between electrical activity and cortical microcirculation revealed by imaging spectroscopy: implications for functional brain mapping. Science 272, 551–554.

Meek, J.H., Firbank, M., Elwell, C.E., Atkinson, J., Braddick, O., Wyatt, J.S., 1998. Regional haemodynamic responses to visual stimulation in awake infants. Pediatric Research 43, 840–843.

Murata, Y., Sakatani, K., Katayama, Y., Fukaya, C., 2002. Increase in focal concentration of deoxyhemoglobin during neuronal activity in cerebral ischemic patients. Journal of Neurology, Neurosurgery and Psychiatry 73, 182–184.

Murata, Y., Sakatani, K., Fujiwara, N., Hoshino, T., Fukaya, C., Yamamoto, T., 2004. Decreases of blood oxygenation level dependent signal in the activated motor cortex during functional recovery after resection of a glioma. AJNR 25, 1242–1246.

Ogawa, S., Lee, T.M., Kay, A.R., Tank, D.W., 1990. Brain magnetic resonace imaging with contrast dependent on blood oxygenation. Proceedings of the National Academy of Sciences of the United States of America 87, 9868–9872.

Ogawa, S., Tank, D.W., Menon, R., Ellermann, J.M., Kim, S.G., Merkle, H., Ugurbil, K., 1992. Intrinsic signal changes accompanying sensory stimulation: functional brain mapping with magnetic resonance imaging. Proceedings of the National Academy of Sciences of the United States of America 89 (1992), 5951–5955.

Parks, R.W., Loewenstein, D.A., Dodrill, K.L., Barker, W.W., Yoshii, F., Chang, J.Y., Emran, A., Apicella, A., Sheramata, W.A., Duara, R., 1988. Cerebral metabolic effects of a verbal fluency test: a PET scan study. Journal of Clinical and Experimental Neuropsychology 10, 565–575.

Patterson, M.S., Chance, B., Wilson, C., 1986. Time resolved reflectance and transmittance for the non-invasive measurement of tissue optical properties. Applied Optics 28, 2331–2336.

Pryds, O., Greisen, G., Skov, L.L., Friis-Hansen, B., 1990. Carbon dioxide-related changes in cerebral blood volume and cerebral blood flow in mechanically ventilated preterm neonates: comparison of near infrared spectrophotometry and 133 Xenon clearance. Pediatric Research 27, 445–449.

Quaresima, V., Ferrari, M., Torricelli, A., et al., 2005. Bilateral prefrontal cortex oxygenation responses to a verbal fluency task: a multichannel time-resolved near-infrared topography study. Journal of Biomedical Optics 10 (1), 11012.

Raichle, M.E., MacLeod, A.M., Snyder, A.Z., Powers, W.J., Gusnard, D.A., Shulman, G.L., 2001. A default mode of brain function. Proceedings of the National Academy of Sciences of the United States of America 98, 676–682.

Reynolds, E.O., Wyatt, J.S., Azzopardi, D., Delpy, D.T., Cady, E.B., Cope, M., Wray, S., 1988. New non-invasive methods for assessing brain oxygenation and haemodynamics. British Medical Bulletin 44, 1052–1075.

Sakatani, K., Xie, Y., Lichty, W., Li, S., Zuo, H., 1988. Language-activated cerebral blood oxygenation and hemodynamic changes of the left prefrontal cortex in poststroke aphasic patients: a near infrared spectroscopy study. Stroke 29, 1299–1304.

Sakatani, K., Saying, C., Wemara, L., Zuo, H., Wang, Y., 1999a. Cerebral blood oxygenation changes induced by auditory stimulation in newborn infants measured by near-infrared spectroscopy. Early Human Development 55, 229–236.

Sakatani, K., Lichty, W., Xie, Y., Li, S., Zuo, H., 1999b. Effects of aging on language-activated cerebral blood oxygenation changes of the left prefrontal cortex: near infrared spectroscopy study. Journal of Stroke and Cerebrovascular Diseases 8, 398–403.

Sakatani, K., Lichty, W., Wang, Y., Zuo, H., Yabu, K., 1999c. Neuronal activity alters local blood flow in brain tumor adjacent to the activating cortex. Journal of Neurology, Neurosurgery and Psychiatry 67, 553–554.

Sakatani, K., Katayama, Y., Yamamoto, T., Suzuki, S., 1999d. Cerebral blood oxygenation changes of the frontal lobe induced by direct electrical stimulation of thalamus and globus pallidus: a near infrared spectroscopy study. Journal of Neurology, Neurosurgery and Psychiatry 67, 769–773.

Tanida, M., Sakatani, K., Takano, R., Tagai, K., 2004. Relation between asymmetry of prefrontal cortex activities and the autonomic nervous system during a mental arithmetic task: near infrared spectroscopy study. Neuroscience Letters 369, 69–74.

Walter, H., Vetter, S.C., Grothe, J., Wunderlich, A.P, Hahn, S., Spitzer, M., 2001. The neural correlates of driving. Neuroreport 13, 1763–1767.

Wolf, M., Wolf, U., Choi, J.H., Toronv, V., Paunescu, L.A., Michalos, A., Gratton, E., 2003. Fast cerebral function singal in the 100-ms range

detected in the visual cortex by frequency-domain near-infrared spectrophotometry. Psychophysiology 40, 521–528.

Zhao, H., Tanikawa, Y., Gao, F., Onodera, Y., Sassaroli, A., Tanaka, K., Yamada, Y., 2002. Maps of optical differential pathlength factor of human forehead, somatosensory motor and occipital regions at multi-wavelengths in NIR. Physics in Medicine and Biology 47, 2075–2093.

Zhang, H., Miwa, M., Urakami, T., Yamashita, Y., Tsuchiya, Y., 1998. Simple subtraction method for determining the mean pathlength traveled by photons in turbid media. Japanese Journal of Applied Physics 37, 700–704.